A MALDI-Mass Spectrometry Imaging method applicable to different formalin-fixed paraffin-embedded human tissues.

Journal:	*Molecular BioSystems*
Manuscript ID:	MB-MET-12-2014-000716
Article Type:	Method
Date Submitted by the Author:	16-Dec-2014

Complete List of Authors:	De Sio, Gabriele; University of Milano Bicocca, Health Sciences, Clinical Proteomics Unit Smith, Andrew; University of Milano Bicocca, Health Sciences, Clinical Proteomics Unit Galli, Manuel; University of Milano Bicocca, Health Sciences, Clinical Proteomics Unit Garancini, Mattia; San Gerardo Hospital, Surgery Chinello, Clizia; University of Milano Bicocca, Health Sciences, Clinical Proteomics Unit Bono, Francesca; University of Milano Bicocca, Surgery and Translational Medicine Pagni, Fabio; University of Milano Bicocca, Surgery and Translational Medicine Magni, Fulvio; University of Milano Bicocca, Health Sciences, Clinical Proteomics Unit

MALDI-Mass Spectrometry Imaging method applicable to different formalin-fixed paraffin-embedded human tissues.

Running title: MALDI-MSI of FFPE human tissues

Gabriele De Sio MS†#, Andrew James Smith MS†#, Manuel Galli MS†#, Mattia Garancini MD*, Clizia Chinello PhD†, Francesca Bono MD**, Fabio Pagni MD** and Fulvio Magni PhD†

†Department of Health Sciences, Clinical Proteomics Unit, University Milan-Bicocca, Milan, Italy,

* Department of Surgery, San Gerardo Hospital, Monza, Italy

**Department of Surgery and Translational Medicine, Pathology, University Milan-Bicocca, Monza, Italy,

# equally contributor authors

Conflict of interest statement: The authors declare that there are no conflicts of interest

Corresponding author:

Fabio Pagni, MD

**Department of Surgery and Translational Medicine,

Section of Pathology

University Milan Bicocca

Monza, Italy,

Email: Fabio.pagni@unimib.it

ABSTRACT

Recent advancements in Matrix Assisted Laser Desorption/Ionisation (MALDI) Mass Spectrometry Imaging (MSI) technology have enabled the analysis of formalin-fixed paraffin-embedded (FFPE) tissue samples, unlocking a wealth of new proteomic information and facilitating the possibility of performing studies with higher statistical power as well as multi-centric collaborations within the field of proteomics research. However, current methods used to analyse these specimens are often time-consuming and they need to be modified when applied to human tissue of different origin. Here we present a reproducible and time-effective method that could address these aforementioned issues and widen the applicability of this technology to a number of challenging tissue types. Additionally, tissue molecular images show high spatial resolution and a strong correlation with the morphological features, enabling the identification of tissue morphology using statistically derived visualisation, without any prior knowledge.

Keywords (3-8): PROTEOMICS; MALDI-MSI, IMAGING MASS SPECTROMETRY; FFPE

INTRODUCTION

Matrix Assisted Laser Desorption/Ionisation Mass Spectrometry Imaging (MALDI-MSI) has a high potential in providing clinical translational applications for disease-related protein identification, especially in histopathology. Indeed, MALDI-MSI is commonly used to visualise the spatial distribution of proteins and peptides in pathological tissue sections directly *in-situ*, matching specific morphological criteria with exact localisation. It can also target a number of other analytes including lipids, metabolites and xenobiotics.

This proteomic technique was traditionally developed for the analysis of fresh-frozen tissue sections[1,2] and it has been successfully used in preclinical and clinical investigations showing a variety of applications in several fields such as oncology[3], degenerative disorders[4] and immunological diseases[5,6]. Different types of tissue have been used in these studies, including brain, breast, ovarian, prostate, gastrointestinal and kidney. Interestingly, recent pilot studies have also applied this methodology to samples different from fresh-frozen tissue, such as cytological smears[7,8], widening the scope of this type of analysis. However, since all these specimens require fresh material, MALDI-MSI has been limited to centres containing both MALDI mass spectrometers as well as their own pathology department, which are required in order to avoid the sample degradation that may occur during shipment unless very stringent and expensive methods are followed. Consequently, the recruitment of a number of patients sufficient to increase the robustness of the outcome has become a challenging aspect of clinical studies focused on MALDI MSI[9].

The most promising strategy for overcoming these limitations for proteomic analyses could be represented by formalin-fixed paraffin-embedded (FFPE) tissue, allowing access to large collections of clinically annotated samples and enabling the tissue preservation of samples when stored at room temperature for long periods. Despite these advantages, the application of MALDI-MSI is much more troublesome than with fresh-frozen tissue. More specifically, the analysis of FFPE tissue requires a more complex and time-consuming sample preparation, limiting the

widespread use of this methodology in proteomics research, with deparaffinisation, rehydration, antigen retrieval and enzymatic digestion representing the most important FFPE-specific issues[10]. Although general methods applicable to different tissue types have been suggested[11], several parameters should often be optimised specifically for each different tissue in order to achieve usable results[12,13,14].

Therefore, we propose a reproducible and easy-to-perform strategy that fulfils the requirement of a generic method for the MALDI-MSI analysis for human FFPE specimens and performs optimally with tissue of different origin.

MATERIAL AND METHODS

The study was conducted on left-over material according to the local Ethical Board rules; FFPE blocks of different human tissues were taken from the archive of the Department of Pathology, San Gerardo Hospital, Monza, Italy. Tissues were fixed according to standard routine methods, with a timing of 24 to 48 hours for surgical specimens. For autoptic samples, no rigorous standardisation was applied and the fixation time ranged between 24 hours and 5 days. After the fixation phase, inclusion was performed using an automatic Tissue Processing Centre (TPC 15 Duo/Trio, Medite, MeBurgdorf, German). Different human tissues specimens were chosen to evaluate the analytical method. The selection of specimens included human brain, cerebellum and cerebral cortex, from autopsy; normal kidney from nephrectomy specimens performed for neoplasia; normal thyroid residual from multinodular goiter and normal small bowel from pancreasectomy for ductal adenocarcinoma. For each block, 5 micron thick sections were cut and mounted on conductive Indium Tin Oxide (ITO)-glasses. The slides were stocked at room temperature until the day of the analysis. Each slide was treated using a method (A) derived from published studies[15,16] and with our method (B).

Method A: slides were washed twice for 5 min with high performance liquid chromatography (HPLC) grade xylene; then for 5 min with EtOH (90-70-50-30 %) followed by 10mM ammonium

bicarbonate buffer (twice for 3 min); the antigen retrieval was performed in a bath of 20mM Tris-HCl buffer, pH 9 at 97°C for 30 min.

Method B: slides were first left in the oven for 1 hour at 65°C then washed three times for 2 min with high performance liquid chromatography (HPLC) grade xylene; then with 100% EtOH (twice for 3 min); with 70% EtOH (once for 3 min)**;** and with HPLC grade H_2O (twice for 2 min); the antigen retrieval was performed in a bath of 10mM citric acid buffer at 97°C for 30 min followed by 2 min in a histology glass container with HPLC grade H_2O.

Afterwards, trypsin deposition (Sigma-Aldrich, Chemie Gmbh, Steinheim, Germany, 100 ng/µl) was performed using the ImagePrep (Bruker Daltonics, Bremen, Germany) automated spraying system and then left in a humid chamber for 2 hours at 45°C for method B instead of the approximate 3 hours at 37°C used for method A. Finally, matrix deposition for MALDI analysis was performed by spraying Cyano-4-hydroxycinnamic acid (7 mg/ml) using the ImagePrep (Bruker Daltonics, Bremen, Germany).

All the mass spectra were acquired in reflectron positive mode in the mass range of 800 to 4000 *m/z* (approximately 9000 spectra per tissue section) with the UltrafleXtreme mass spectrometer (Bruker Daltonics, Bremen, Germany). Spectra were collected with a laser diameter of 50 micron and an 80 micron raster. After MALDI analysis, the matrix was removed with increasing concentrations of EtOH (70% and 100%) and the slides stained with Haematoxylin & Eosin. The slides were converted to digital format by scanning through the ScanScope CS digital scanner (Aperio, Park Center Dr. Vista, CA, USA), thus allowing the direct overlap of images and the integration of proteomic and morphologic data. FlexImaging 3.0 (Bruker Daltonics, Bremen, Germany) data, containing spectra of each entire measurement region, were imported into SCiLS Lab 2014 software (http://scils.de/; Bremen, Germany) after the acquisition. SCiLS was used to perform a series of pre-processing steps on the loaded spectra: baseline subtraction (TopHat algorithm[17]) and normalisation (Total Ion Current algorithm[18]). A series of further steps were performed in order to generate an average (avg) spectrum representative of the whole measurement region: peak picking (Orthogonal

Matching Pursuit algorithm[19]), peak alignment (to align the detected ions with peak maxima[20,21]) and spatial denoising (http://scils.de/; SCiLS Lab; 8.8 Spatial Denoising). Reproducibility of methods were evaluated based on number of ions, variance and standard deviation of their intensity. Moreover, Principal Component Analysis (PCA) and Hierarchical Clustering (HC), in particular using the bisecting K-means algorithm, were also performed. Spectra showing comparable features were grouped under the same node and then selected and assigned a specific colour based upon their similarity. Each colour was assigned to a group of pixels and used to generate an image representative of the tissue sections.

RESULTS

The main aim of the study was to set up a reproducible and easy-to-perform method useable with different human tissues of different origin, procession (autopsy and surgery) and fixation time[17]. Firstly, the proposed method (B) was compared to the one derived from literature (method A) using human brain and thyroid specimens. Then, the analytical features of the proposed method were evaluated in order to ensure the robustness of the method with other human tissue: kidney and small bowel.

Comparison of Methods

The method derived from published studies (method A) and the modified version (method B) were initially compared using human brain sections, one of the most heterogeneous and challenging samples, and then using thyroid tissue. The average spectra of the two different areas of human brain, cerebellum and cortex, showed a remarkable difference between the two methods, as visualised in Figure 1 (left and middle panels).

The majority of the ions (*m/z*) had an enhanced intensity when using method B in comparison with method A. These differences can be better evaluated in the zoomed spectra (Figure 1; middle panels). For most of the signals (*m/z*), such as those shown in figure 1 (right panels), the low intensity in samples prepared with method A could hamper the acquisition of the MS/MS spectra.

The number of signals in the average mass spectrum of the whole sections and of the different histological areas within the cerebral cortex and cerebellum (inner glia, granular layer, molecular layer, white and grey matter and meninges) was always higher with method B than with method A (Table 1), independently from the considered mass range (Figure 2).

Indeed, not only was the signal intensity higher with method B than with method A but also the signal-to-noise ratios were better, as shown by using the five most intense signals (Table 1).

Similarly, in thyroid specimens, we detected more than 500 signals with method B and approximately 250 with method A. Additionally, the signals detected with method B also had a higher intensity and signal-to-noise ratio (Table 1).

Spatial distribution

To investigate whether method B does not promote protein/peptide delocalisation, molecular images of the human cerebellum were generated using peptides with different localisation, but specific for particular morphological regions, and compared with those derived from method A, as shown in figure 3 (MALDI-MS molecular images). The spatial distribution of peptides at *m/z* 872, 1051, 1421 and 1744 in the cerebellum and cerebral cortex enables the generation of well-defined molecular images that correlate with areas of specific morphology using method B but not with method A, as highlighted in figure 3.

To further investigate the potentiality of method B, we submitted the entire dataset of mass spectra of these two tissues to Hierarchical Cluster Analysis (HCA) in blind mode. The HCA classified spectra based upon their similarities, under specific nodes, and generated a colour-coded image correlating with these nodes (Figure 3, right column, HCA). The generated clusters of spectra successfully classified regions of the external molecular layer of cerebellum cortex, the granular layer and the inner glia with a notable improvement in image resolution using data belonging to method B compared with method A. These findings were also confirmed in the cerebral cortex. Additionally, in specimens analysed with the proposed method, a cluster of spectra that could be associated with the meninges were also observed.

MALDI-Imaging with different human tissues

Based on the encouraging results obtained with brain (cerebellum and cortex) and thyroid tissue using the modified method (B), we investigated its performance with other tissues with different cellular composition: normal kidney and duodenum. For this purpose, three sections of each specimen were prepared with method B and analysed. Average spectra obtained from each of the different tissue types by the application of this method are shown in figure 4. A high number of signals (approximately 300 per each specimen, similar to brain tissue) of high relative intensity were also obtained for these tissues (Table 2). Additionally, almost all of the ions present in the spectra were within the 800-2500 *m/z* range with only a few signals above *m/z* 3000, thus suggesting that complete digestion had occurred within the 2-hour incubation period. Finally, different proteomic profiles were observed for each tissue type.

Reproducibility

The analytical variability of method B was evaluated by analysing three consecutive sections of each tissue type in three different days and by three different operators. Results showed a reproducible number of ions detected for all specimens in the three analytical sections with an average number of approximately 300 signals for all specimens, and with a standard deviation of the intensity for all ions present in the mass spectra always below 10%. (Table 2). A particularly higher number (more than 500 ions) were obtained for the thyroid tissues.

An example of results obtained in the three consecutive days of analysis for normal human cerebellum is shown in figure 5. The average number of signals present in the three spectra was 303 ± 10, with all the standard deviations of their intensity below 7%, underlining a good level of reproducibility (Figure 5a). To further strengthen these findings, PCA was performed on the entire dataset (~25,000 spectra), with each point on the PCA score chart representing an individual spectrum (Figure 5b). The homogeneous and concentric distribution, along with the absence of isolated clusters within the dataset emphasises the low variability between the three experiments.

DISCUSSION

Recently, numerous groups have published successful methods for the management of FFPE tissue for MALDI-MSI analysis[11-17] and several reviews have outlined the challenging points of these procedures[16,22]. However, these methods are generally evaluated using only one type of tissue sample, with no comparison between different biological specimens, and they usually require further specific optimisation depending upon the tissue type. The method described here is easy-to-perform, reproducible and could be useful in the analysis of different FFPE tissue. Moreover, the method is more time-effective, taking on average no longer than 4-5 hours to prepare a tissue section for MALDI-MSI. The performance of this method was evaluated, using features such as the number of signals, the signal-to-noise ratio, the intensity of the five most abundant ions and molecular images, and was shown to be enhanced when compared to the method derived from previous studies (Table 1).

Some modifications to the recently published methods[4-6] seem to be relevant in order to widen its application. Three critical steps were addressed in this method: paraffin removal, antigen retrieval and on-tissue digestion with trypsin. Firstly, more efficient deparaffinisation and tissue adhesion could be achieved by placing the glass slides in an oven at 65°C for an hour prior to washing with xylene. As a result, the total washing time with xylene is greatly diminished and the efficacy enhanced, also preventing tissue distortion due to long-term xylene immersion. The second crucial step regards the fixation. Although the reaction of formaldehyde with basic amino acid residues, such as arginine or lysine, preserves tissue integrity and cellular constituents, the formation of these methylene bridges alters the three-dimensional configuration of the proteins and leads to inefficient protein recovery[11]. This protein cross-linking can be overcome through the process of antigen retrieval, resulting in the unmasking of epitopes and partial unfolding of proteins. During the antigen retrieval phase, the combination of citric acid buffer with a gradual increase and decrease in temperature at the start and end of the phase avoids thermal shock and damage to the tissue structure. Moreover, we examined tissues of different origin with our method (both autoptic and

bioptical specimens). The results obtained with all the investigated specimens highlighted that the proposed method is reproducible, irrespective of the origin of the tissue (Table 2). In order to be detectable via MALDI-MSI, proteins present in FFPE tissue must be digested, most commonly enzymatically using trypsin. Our incubation step during tryptic digestion has been reduced to only 2 hours and was shown to be sufficient for use with tissue of varying origin and fixation time (Figure 4). Moreover, one of the major problems attributed to trypsin deposition is the delocalisation of peptides, being a strong aqueous based step. Results highlighted that our protocol well preserved the spatial distribution of the analytes, enabling the visualisation of different peptides with localisation related to different morphological features (Figure 3). This could potentially be a result of the reduced incubation time for tryptic digestion, ensuring that the tissue remains in a humid atmosphere for the minimum amount of time possible, along with a successful enzymatic process. Generally, the proposed method is both time (4 hours for a complete experiment) and cost-effective as well as being able to provide mass spectra of high quality with different specimens prepared with different fixation time (Figure 4). In particular, we chose tissue types that are particularly challenging for proteomic analysis, such as lipid-rich nervous tissue of cerebellum and cerebral cortex, highly hemoglobin-rich kidney sections, colloid-embedded thyroid follicles and visceral organs with a succession of overlapping layers such as mucosa, submucosa, muscularis and peritoneum.

In each of these cases, the mass spectra were of the same high quality (high number of ions with a higher relative intensity) and displayed significantly different proteomic profiles which could potentially be used to classify sub-areas of tissue of pathological interest. Additionally, we have also highlighted that our protocol is highly reproducible, even when performed by different operators (Figure 5). More interestingly, by submitting the raw data of the entire dataset in blind to HCA, it was possible to successfully distinguish regions of tissue based upon their spectral differences, even in instances where these regions are very small but also potentially significant (Figure 4, yellow spots on the meninx vessels). Additionally, great benefits could be derived from

the application of our method to other proteomic strategies such as on-tissue MS/MS, due to the higher ion intensity (Figure 1, right panel), and nanoLC-ESI-MS/MS with a micro-extraction strategy[23] due to the peptide localisation within the tissue being preserved. These techniques could enable the attainment of information regarding the identity of proteins detected in FFPE tissue which can act as biological markers of disease, providing diagnostic, prognostic and potentially therapeutic significance.

ACKNOWLEDGMENTS

This work was supported by grants from the MIUR: FIRB 2007 (RBRN07BMCT_11), FAR 2010–2013; from i-MODE-CKD (FP7-PEOPLE-2013-ITN) and in part by the EuroKUP COST Action (BM1104) Mass Spectrometry Imaging: New Tools for Healthcare Research.

REFERENCES

1 Caprioli RM, Fermer TB, Gile J. Molecular imaging of biological samples: localization of peptides and proteins using MALDI-TOF MS. Anal. Chem. 1997; 69: 4751-4760

2 Mainini V, Pagni F, Ferrario F, et al. MALDI imaging mass spectrometry in glomerulonephritis: feasibility study. Histopathology. 2014;64(6):901-6

3 Gemoll T, Roblick UJ, Habermann JK. MALDI mass spectrometry imaging in oncology. Mol Med Rep. 2011;4(6):1045-51

4 Hanrieder J, Phan NT, Kurczy ME, Ewing AG. Imaging mass spectrometry in neuroscience. ACS Chem Neurosci. 2013;4(5):666-79

5 Lalowski Magni F, Mainini V, et al. Imaging mass spectrometry: a new tool for kidney disease investigations. Nephrol Dial Transpl 2013; 28(7):1648-56

6 Neubert P, Walch A. Current frontiers in clinical research application of MALDI imaging mass spectrometry. Expert Rev Proteomics. 2013;10(3):259-73

7 Pagni F, Mainini V, Garancini M, et al. Proteomics for the diagnosis of thyroid lesions: preliminary report. Cytopathology. 2014 Jul 20. doi: 10.1111/cyt.12166

8 Mainini V, Pagni F, Garancini M et al. An alternative approach in endocrine pathology research: MALDI-IMS in papillary thyroid carcinoma. Endocr Pathol. 2013;24(4):250-3

9 Dekker TJ, Balluff BD, Jones EA, et al. Multicenter Matrix-Assisted Laser Desorption/Ionization Mass Spectrometry Imaging (MALDI MSI) Identifies Proteomic Differences in Breast-Cancer-Associated Stroma. J Proteome Res. 2014 May 2 (Epub ahead of print)

10 Gorzolka K, Walch A. MALDI mass spectrometry imaging of formalin-fixed paraffin-embedded tissues in clinical research. Histol Histopathol. 2014 (Epub ahead of print)

11 Casadonte R, Caprioli RM. Proteomic analysis of formalin-fixed paraffin-embedded tissue by MALDI imaging mass spectrometry. Nat Protoc. 2011;6(11):1695-709.

12 Ronci M, Bonanno E, Colantoni A, et al. Protein unlocking procedures of formalin-fixed paraffin-embedded tissues: application to MALDI-TOF imaging MS investigations. Proteomics. 2008;8(18):3702-14.

13 Franck J, Arafah K, Elayed M et al. MALDI imaging mass spectrometry: state of the art technology in clinical proteomics. Mol. Cell. Proteomics 2009; 8: 2023–2033.

14 Casadonte R, Kriegsmann M, Zweynert F, et al. Imaging mass spectrometry to discriminate breast from pancreatic cancer metastasis in formalin-fixed paraffin-embedded tissues. Proteomics. 2014;14(7-8):956-64

15 Lemaire R, Desmons A, Tabet JC, Day R, Salzet M, Fournier I. Direct Analysis and MALDI Imaging of Formalin-Fixed, Paraffin-Embedded Tissue Sections. J. Proteome Res. 2007, 6, 1295.

16 Fowler CB, O'Leary TJ, Mason JT. Toward improving the proteomic analysis of formalin-fixed, paraffin-embedded tissue. Expert Rev Proteomics 2013 10, 389.

17 Powers TW, Neely BA, Shao Y. MALDI Imaging Mass Spectrometry Profiling of N-Glycans in Formalin-Fixed Paraffin Embedded Clinical Tissue Blocks and Tissue Microarrays. PLoS One. 2014;9(9):e106255.

18 Deininger SO, Cornett D, Paape R et al. Normalization in MALDI-TOF imaging data sets of proteins: practical considerations. Analytical and Bioanalytical Chemistry 2011, 401:167-181

19 Alexandrov T, Becker M, Deininger SO et al. Spatial segmentation of imaging mass spectrometry data with edge-preserving image denoising and clustering. Journal of Proteome Research 2010, 9:6535-6546.

20 Alexandrov T, Kobarg JH Efficient spatial segmentation of large imaging mass spectrometry data sets with spatially aware clustering. Bioinformatics 2011, 27(13):i230-i238

21 Alexandrov T, Meding, S, Trede D et al. Super-resolution segmentation of imaging mass spectrometry data: Solving the issue of low lateral resolution. Journal of Proteomics 2011, 75:237-245

22 Hood BL, Conrads TP, Veenstra TD. Mass spectrometric analysis of formalin-fixed paraffin-embedded tissue: unlocking the proteome within. Proteomics. 2006 Jul; 6(14): 4106-14.

23 Quanico J, Franck J, Dauly C, Strupat K, Dupuy J, Day R, Salzet M, Fournier I, Wisztorski M. Development of liquid microjunction extraction strategy for improving protein identification from tissue sections. J Proteomics. 2013 Feb 21;79:200-18.

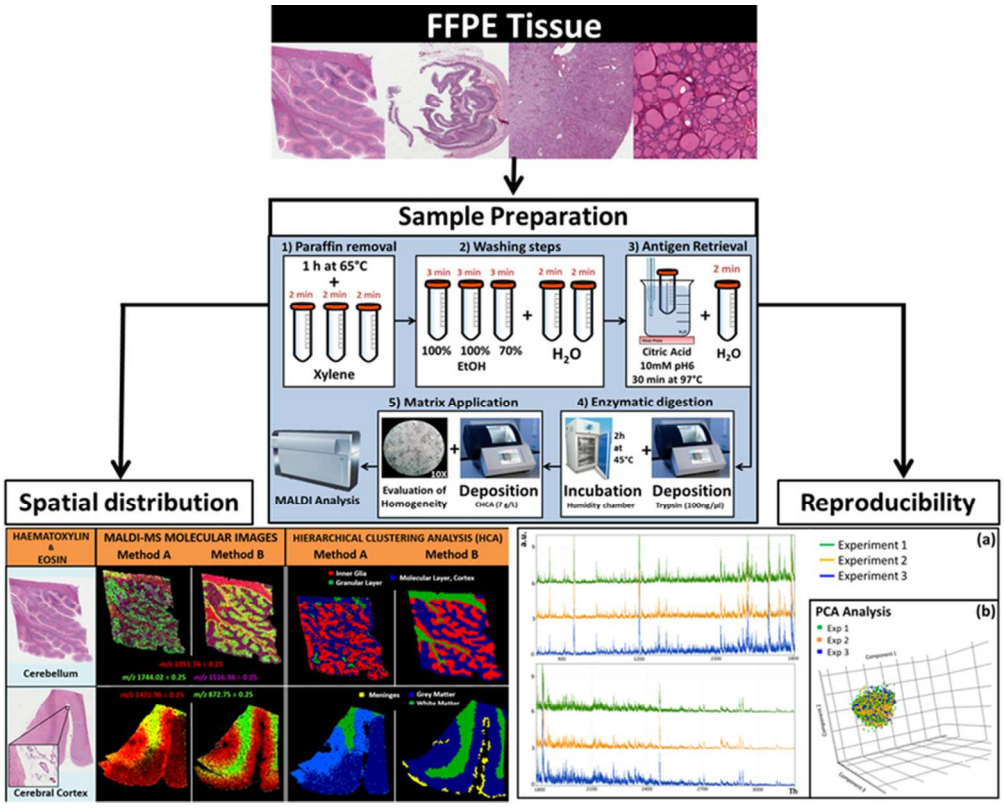

34x27mm (600 x 600 DPI)

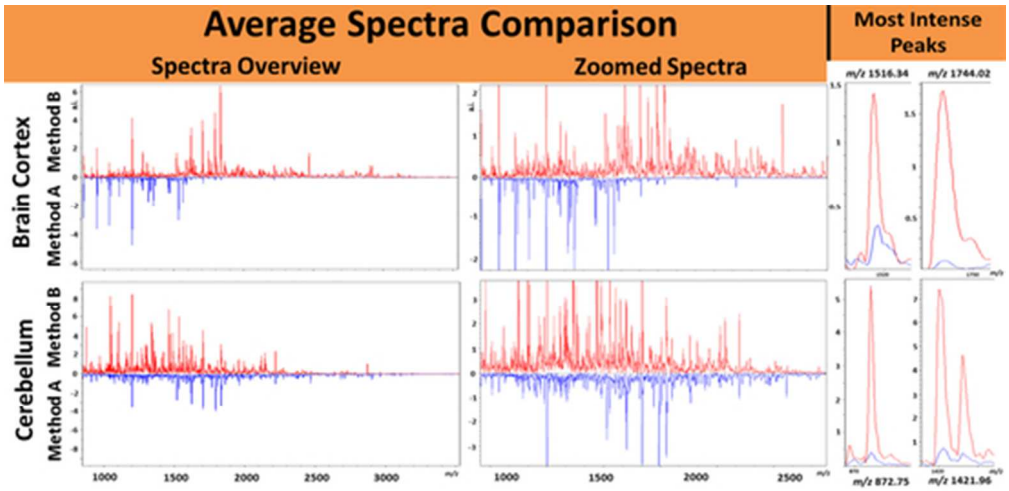

Figure 1: Comparison of Method A (blue) and Method B (red) using average spectra obtained from brain cortex (top) and cerebellum (bottom). The differences are highlighted using the overview spectra (left panel), the zoomed spectra (central panel) and ions with a particular spatial localisation in Cerebral cortex (m/z 1516, m/z 1744) and Cerebellum (m/z 872, m/z 1421), respectively (right panel).
23x11mm (600 x 600 DPI)

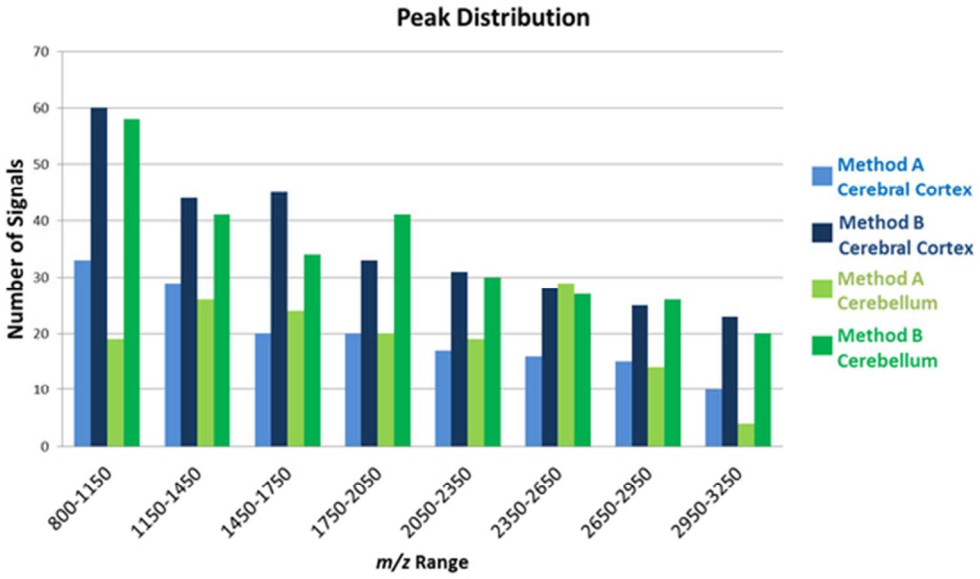

Figure 2: Distribution of the number of ions detected in different mass ranges across the average mass spectra obtained from cerebral cortex and cerebellum, comparing Method A with Method B.
26x15mm (600 x 600 DPI)

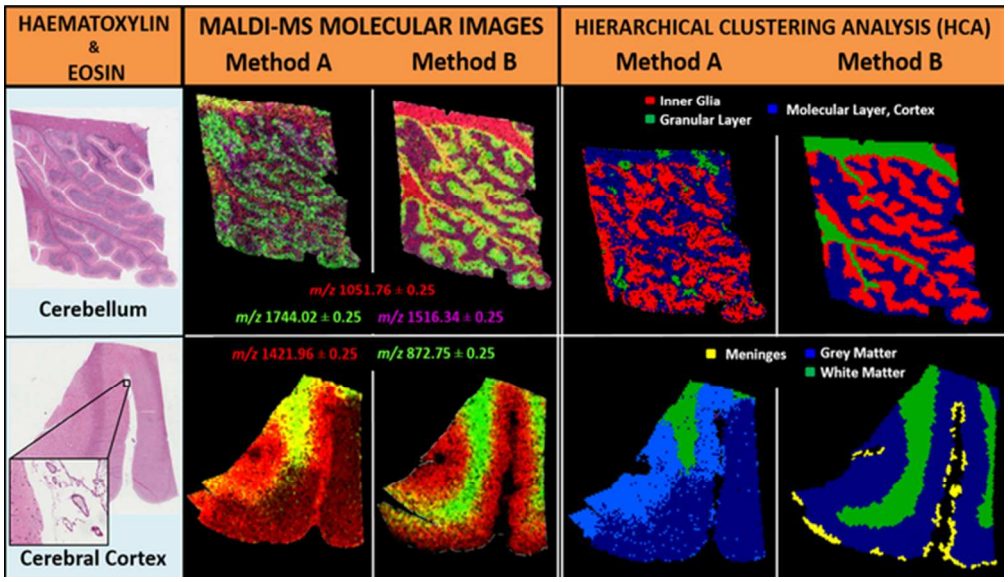

Figure 3. MALDI-MSI analysis of human brain FFPE tissue. Hematoxylin & Eosin stained images of tissue sections taken from human cerebellum and cerebral cortex (left). Examples of MALDI-MS images of peptides localised to distinct morphological regions of the brain, shown as an overlay, and used to visualise the entire section (centre). Visualisation of the hierarchical clustering analysis, indicating the spectral similarities (represented as colour-coded pixels) are correlated with morphological regions of the brain (right): molecular layer, cortex (blue), the granular layer (green) and the inner glia (red) for the cerebellum and grey matter (blue) and white matter (green) for the cerebral cortex. In the cerebral cortex specimens a cluster of spectra are associated with the meninges (yellow).
28x16mm (600 x 600 DPI)

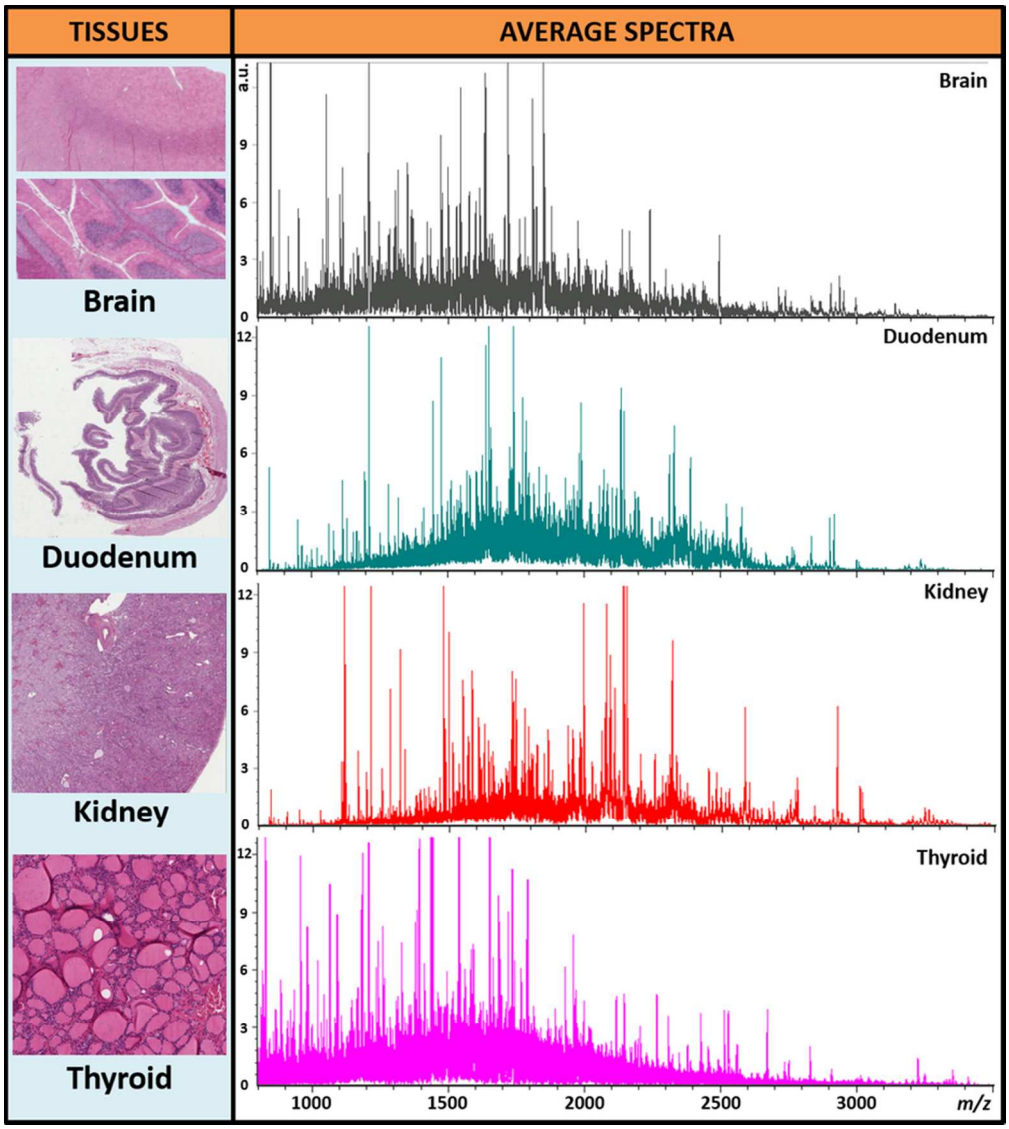

Figure 4. Comparison of the average spectra of human brain, duodenum, kidney and thyroid. On the left, Hematoxylin & Eosin staining of the aforementioned tissue sections derived from FFPE blocks. On the right, average spectra obtained from each tissue type, shown in the mass range of 800 to 3500 m/z. The intensity of the signals is expressed in arbitrary units (a.u.).
39x44mm (600 x 600 DPI)

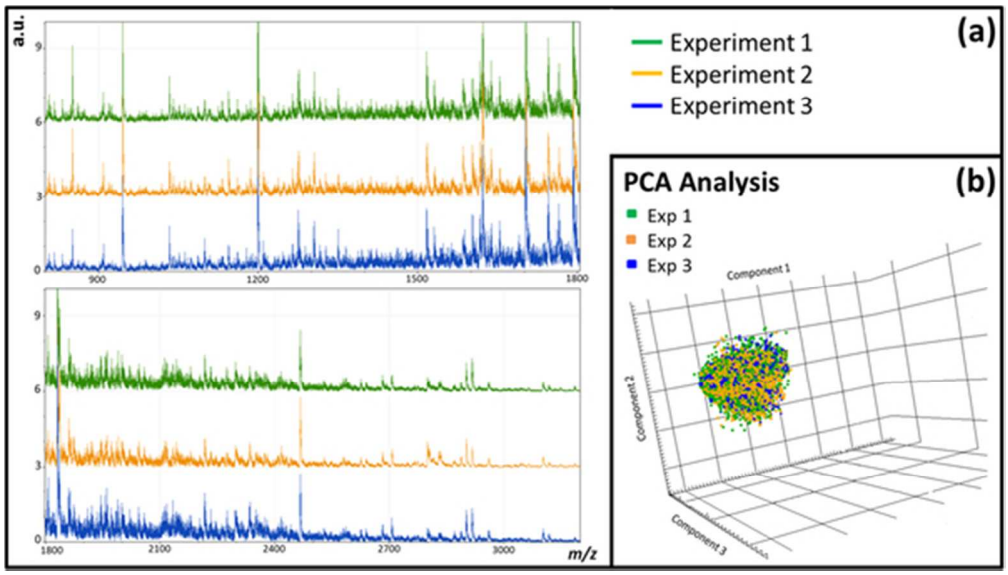

Figure 5. Average mass spectra obtained by analysing three consecutive sections of human cerebellum independently. a) Zoomed regions of spectra in the mass range of 800 to 1800 m/z (top) and 1800 to 3500 m/z (bottom). b) Variability present within the data as represented by a three-dimensional PCA score chart incorporating the entire dataset, with each pixel representing an individual spectrum (green: experiment 1; orange experiment 2, blue: experiment 3).
25x14mm (600 x 600 DPI)

Tissue	n° of peaks in the Avg. Spectrum		S/N range of the five most intense peaks		Intensity range of the five most intense peaks	
	A	B	A	B	A	B
Cerebellum	155	292	23 - 33	32 - 60	1.8 - 4.9	4.2 - 8.6
Inner glia	128	286				
Granular layer	136	291				
Molecular layer	129	282				
Brain Cortex	160	289	15 - 29	45 - 62	2.7 - 3.9	4.9 - 7.5
White matter	185	316				
Grey matter	171	301				
Meninges	0	310				
Thyroid	256	570	20 – 26	30 – 69	3.7 – 5.1	7.4 – 9.2

Table 1: Overview of the number of ions (peaks; m/z) detected in the average spectrum of cerebellum, brain cortex and their sub-regions and thyroid using Method A (A) and Method B (B) along with the signal-to-noise ratio and intensity (expressed as arbitrary intensity, a.i.) ranges of the five most intense ions detected in the average spectrum of cerebellum, brain cortex and thyroid.
24x14mm (600 x 600 DPI)

Tissue	Experiment 1 n° of Peaks	Experiment 2 n° of Peaks	Experiment 3 n° of Peaks	Avg n° of Peaks	StDev (% peak intensity)
Cerebellum	314	299	295	303	<7%
Cerebral Cortex	315	282	296	298	<10%
Thyroid	577	552	596	575	<8%
Kidney	283	264	268	272	<3%
Cortex	344	360	317	340	<9%
Medulla	328	349	356	344	<3%
Duodenum	320	296	286	301	<4%

Table 2: Number of ions (peaks; m/z) detected, the average number and the standard deviation of their intensity in different sections of human FFPE tissue obtained from the three different analytical assays.
20x9mm (600 x 600 DPI)

Figure 1: Comparison of Method A (blue) and Method B (red) using average spectra obtained from brain cortex (top) and cerebellum (bottom). The differences are highlighted using the overview spectra (left panel), the zoomed spectra (central panel) and ions with a particular spatial localisation in Cerebral cortex (*m/z* 1516, *m/z* 1744) and Cerebellum (*m/z* 872, *m/z* 1421), respectively (right panel).

Table 1: Overview of the number of ions (peaks; *m/z*) detected in the average spectrum of cerebellum, brain cortex and their sub-regions and thyroid using Method A (A) and Method B (B) along with the signal-to-noise ratio and intensity (expressed as arbitrary intensity, a.i.) ranges of the five most intense ions detected in the average spectrum of cerebellum, brain cortex and thyroid.

Figure 2: Distribution of the number of ions detected in different mass ranges across the average mass spectra obtained from cerebral cortex and cerebellum, comparing Method A with Method B.

Figure 3. MALDI-MSI analysis of human brain FFPE tissue. Hematoxylin & Eosin stained images of tissue sections taken from human cerebellum and cerebral cortex (left). Examples of MALDI-MS images of peptides localised to distinct morphological regions of the brain, shown as an overlay, and used to visualise the entire section (centre). Visualisation of the hierarchical clustering analysis, indicating the spectral similarities (represented as colour-coded pixels) are correlated with morphological regions of the brain (right): molecular layer, cortex (blue), the granular layer (green) and the inner glia (red) for the cerebellum and grey matter (blue) and white matter (green) for the cerebral cortex. In the cerebral cortex specimens a cluster of spectra are associated with the meninges (yellow).

Figure 4. Comparison of the average spectra of human brain, duodenum, kidney and thyroid. On the left, Hematoxylin & Eosin staining of the aforementioned tissue sections derived from FFPE blocks. On the right, average spectra obtained from each tissue type, shown in the mass range of 800 to 3500 *m/z*. The intensity of the signals is expressed in arbitrary units (a.u.).

Table 2: Number of ions (peaks; *m/z*) detected, the average number and the standard deviation of their intensity in different sections of human FFPE tissue obtained from the three different analytical assays.

Figure 5. Average mass spectra obtained by analysing three consecutive sections of human cerebellum independently. a) Zoomed regions of spectra in the mass range of 800 to 1800 *m/z* (top) and 1800 to 3500 *m/z* (bottom). b) Variability present within the data as represented by a three-dimensional PCA score chart incorporating the entire dataset, with each pixel representing an individual spectrum (green: experiment 1; orange experiment 2, blue: experiment 3).